

Henrik Wolfram\*, Johannes Hoffmann, Ralf Burgardt, Eric Elzenheimer, Gerhard Schmidt, and Michael Höft

# PCB Coil Enables In Situ Calibration of Magnetoelectric Sensor Systems

<https://doi.org/10.1515/cdbme-2023-1142>

**Abstract:** Accurate calibration is key for any reliable sensor system. Magnetoelectric (ME) sensors, in particular, are influenced in their operating point by external parameters such as the Earth's magnetic field or the ambient temperature. In this paper, we introduce a new planar coil design for the generation of a magnetic test field within the plane of the ME sensor. Furthermore, we implemented a method for measuring the sensor behaviour using a short-term magnetic noise signal. The combination of the printed circuit board (PCB) coil and the accelerated sensor characterization method allows the sensor system to be calibrated at the measurement site (in situ) without the need for laboratory equipment. We can show that the presented method for calibration achieves high-quality results in 10 seconds for a sensor affected by external interference fields.

**Keywords:** IIR peak filter, magnetoelectric sensors, noise signal, PCB coil, sensor system calibration

## 1 Introduction

The use of ME sensors to determine physical quantities requires precise knowledge of their frequency-dependent sensitivity, which is often described in terms of peak sensitivity, resonance frequency, and bandwidth. All quantities are the result of a complex sensor characterization [1], which typically takes place under controlled laboratory conditions. In applications such as, but not limited to, motion analysis [2] or magnetocardiography (MCG) [3] it is of great importance that the information from the characterization is accurate, as this has a direct influence on the precision of the applied algorithms.

The investigated ME sensor system is based on a 3 x 1 mm cantilever and a low-noise preamplifier. On the top side of the cantilever is a piezoelectric layer and a magnetically sensitive layer. A magnetic field leads to an expansion of the magne-

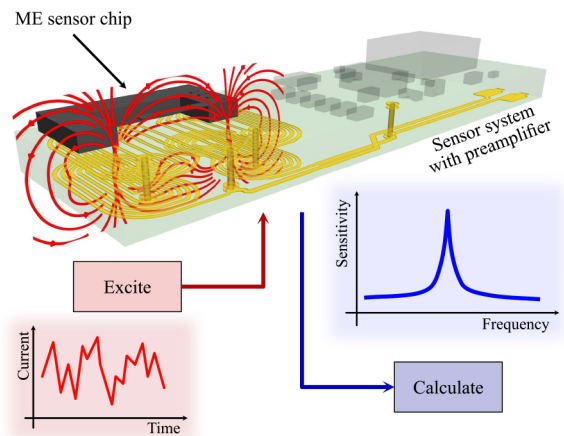


Fig. 1: Schematic description of the on-board calibration.

tostrictive layer that bends the cantilever. A coupled piezoelectric layer converts this strain to an electric voltage.

Based on the functional principle of the sensor, various effects follow that influence the quantities describing the sensor: The magnetic layer is subject to hysteresis effects, our Earth's magnetic field generates a DC bias field that acts on the sensing element, and the ambient temperature also influences the mechanical behaviour of the cantilever [4]. These effects emphasize that it is of great metrological interest to renew the calibration of a sensor system at the place of measurement and thus significantly improve the quality of the measurements performed.

The concept underlying the on-board calibration is illustrated in Fig. 1. A bandlimited noise signal is fed into the PCB coil system. The coils then serve as magnetic field generators optimized to the dimension of the sensing element and with an invariant spatial relationship to it. Therefore, the frequency response of the sensor to the known magnetic signal can be evaluated and derived into a general system description.

## 2 Materials and Methods

In the following section, we discuss the different procedures for characterising and calibrating ME sensors. Sec. 2.1 gives a brief overview of the current state-of-the-art and discusses the conventional method for determining sensor qualities. Then,

\*Corresponding author: Henrik Wolfram, Department of Electrical and Information Engineering, Kiel University, Kaiserstr. 2, 24143 Kiel, Germany, e-mail: hewo@tf.uni-kiel.de  
Johannes Hoffmann, Ralf Burgardt, Eric Elzenheimer, Gerhard Schmidt, Michael Höft, Department of Electrical and Information Engineering, Kiel University, Kiel, Germany

sec. 2.2 is dedicated to the new procedure for on-board calibration, including a description of the new PCB coil design.

## 2.1 State-of-the-art Characterisation

### 2.1.1 System Identification Method

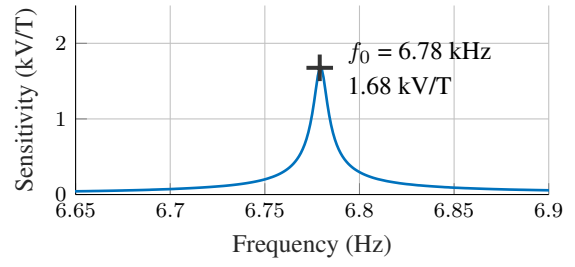
The standard approach for characterizing an ME sensor system currently includes an evaluation of the sensor behavior over a variety of discrete frequencies [1]. This method exploits the suppression property of the delta distribution (spectral representation of the sinusoidal excitation signal) to extract the frequency response at the selected frequency. For this purpose, the sensor system is exposed to a defined and low-noise AC magnetic field, and its voltage amplitude at the output is measured. Since neither the exact resonance frequency of the system nor the quality factor are known a priori, three aspects must be ensured: The measurement time should be long enough to allow the settling of a high-quality resonator. The swept frequency range is large enough to detect the resonance of the sensor. The frequency resolution should be small enough to measure a symmetrical sensitivity curve (Fig. 2a).

### 2.1.2 Experimental Setup

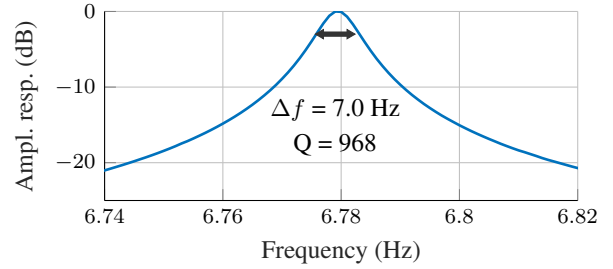
The setup used to determine the sensor system properties includes a magnetic shielding, an AC current source, a lock-in amplifier and a cylindrical coil [5]. An *Aaronia Zero-Gauss-Chamber* ensures the same experimental condition at all times by effectively shielding external magnetic fields. Using a *Keithley 6221* current source and a fully characterized cylindrical coil [6], the sensor system can be exposed to a defined magnetic field. It should be noted, however, that with large cylindrical coils typically only magnetic field frequencies significantly smaller 100 kHz can be generated. Thus, a magnetic characterisation of higher oscillation modes is therefore increasingly infeasible. The detection of the signal at the output of the sensor system is performed with the *SRS SR830* lock-in amplifier, which is frequency synchronised with the current source.

### 2.1.3 Filter Approximation of the Sensor System

Sensitivity in the first mode of the investigated resonant ME sensor is highly frequency-dependent, with peak sensitivity clearly visible at the resonance frequency (cf. Fig. 2a). The maximum sensitivity in terms of a conversion factor can be combined with the bandpass characteristics in terms of a de-



(a) Frequency-dependent sensitivity curve.



(b) Bandpass characteristics of normalized frequency response.

**Fig. 2:** Typical sensor characterization results.

defined bandwidth  $\Delta f$  (e.g., at  $-3$  dB) or the corresponding quality factor  $Q$  to describe the sensor's amplitude response in the region of interest (Fig. 2b). Consequently, reconstructing undistorted magnetic signals from the sensor's output relies on an appropriate equalizer filter. Second-order IIR peak filter designs based on the described parameters have been previously used for equalizing purposes in magnetic motion sensing of ME sensors [2].

## 2.2 In Situ Calibration

### 2.2.1 System Identification Method

While the sine-sweep approach is well-established in magnetic sensor characterization, system theory provides other options. The frequency response  $H$  of a time-discrete system is equivalent to the cross power spectral density between input and output signal  $S_{vy}$  divided by the auto power spectral density of the input signal  $S_{vv}$ . For a white noise input signal of power  $\sigma_v^2$  this yields:

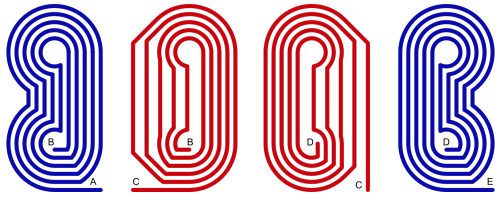
$$H(e^{j\Omega}) = \frac{S_{vy}(\Omega)}{S_{vv}(\Omega)} = \frac{S_{vy}(\Omega)}{\sigma_v^2}. \quad (1)$$

This relation is commonly exploited in system identification and was applied here to estimate the frequency response  $\hat{H}$  of the ME sensor system. The accuracy of this method is dependent on the invested energy as a product of signal power and acquisition time. Short-time estimations of the involved power

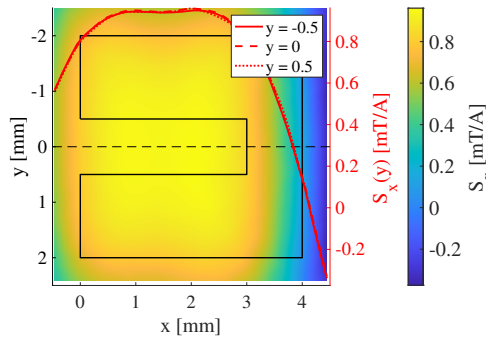
spectra were obtained by averaging multiple flat-top windows (overlap: 50 %) of length 1 s according to Welch's method.

### 2.2.2 Experimental Setup

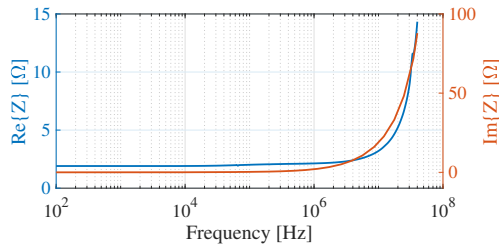
(a) Photograph of a complete ME sensor system.



(b) Four individual coils below the sensor. Red are the upper and blue the lower coils. The letters mark the connection points of the individual coils.



(c) Simulation of the magnetic field within the sensor plane.



(d) Impedance measurement of the PCB coil system.

**Fig. 3:** Visuals and characterisation of the PCB Coil.

In contrast to the measurement of the sensor behaviour using a cylindrical coil described in Sec. 2.1.2, we use the

space available in the PCB below the sensor chip to generate the magnetic field. A photograph of the sensor chip with preamplifier and coils is shown in Fig. 3a. The complex coil design consisting of four different coils (Fig. 3b) distributed on two circuit levels and connected in series makes it possible to generate a homogeneous magnetic field in the sensor plane [7]. Therefore, the two upper coils, which are closer to the sensing element, are designed in such a way that the resulting field is guided as flat as possible along the PCB surface. Both lower coils are designed to contribute a maximum to the resulting field without compromising the homogeneity in the area of interest. A magnetic field simulation in the sensor plane performed using *CST Studio* can be seen in Fig. 3c. The area of interest is that of the cantilever. This ranges in the x-direction from 0 to 3 mm and in the y-direction from  $-0.5$  to  $0.5$  mm. The impedance measurement shown in Fig. 3d as well as noise measurements suggest that the magnetic field generator constructed in this way can be approximated as an ohmic resistor up to a frequency of 1 MHz. In addition, the coil design, due to its two almost symmetrical sets with opposite winding senses, is extremely resistant to external interference. The electrical behaviour and the small distance between the coils and the sensing element ensure that sufficiently large test signals can be generated using signal generators such as sound cards and simple voltage amplifiers.

### 2.2.3 Filter Approximation of the Sensor System

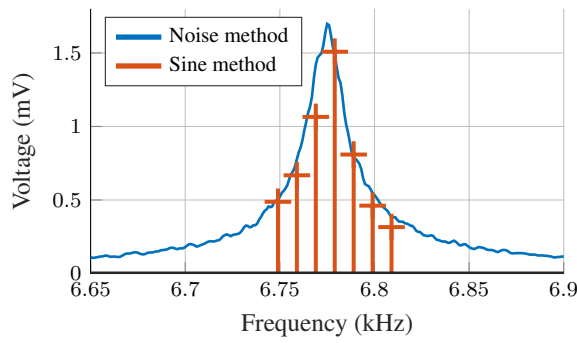
Filter design based on the estimated frequency response was performed similar to the sine excitation method. First, the resonance peak with the corresponding conversion factor was identified, then the  $-3$  dB points were obtained from the normalized and smoothed frequency response (moving average filter, window length: 5 Hz).

## 2.3 Signal Amplitude Calibration

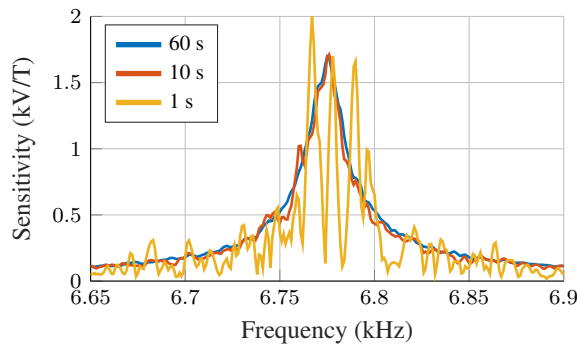
As the magnetic field is related to the current and not the voltage fed to the PCB coil, we applied a calibration (current source and reference coil) at  $1 \mu\text{T}$ . Then, we calculated the required voltage for the PCB coil to reach the equivalent magnetic field, which was 339 mV.

## 3 Results

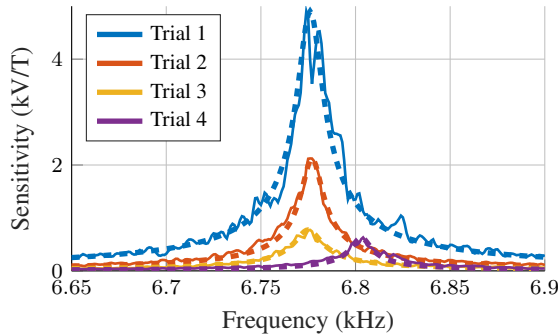
Fig. 4a draws the comparison between the amplitude response estimation from noise excitation and the discrete supporting



(a) Validation of the presented approach with the reference coil.



(b) Sensitivity curve estimation with varying acquisition time.



(c) Filter design based on estimated parameters.

**Fig. 4:** Measurement results for investigated test scenarios.

points at specific frequencies obtained with the reference sine source. These results correspond to the RMS output voltage of the sensor in terms of an amplitude spectrum (without normalisation of the input signal).

Fig. 4b highlights the decrease in result quality of the estimated frequency response for a reduced acquisition time, which starts to deviate heavily below 10 s.

Fig. 4c illustrates qualitative variations in the sensitivity curve when the sensor was exposed to parasitic fields (in this example, a permanent magnet). The previously estimation (10 s, normal line) and filter design method (dashed line) were applied in each exemplary trial.

## 4 Conclusion

In this paper, we investigated a novel characterisation method for magnetoelectric sensors utilizing an on-board magnetic field generator and a noise characterisation scheme. Based on visual inspection, the results obtained via the in situ measurement method are in high agreement with the results from a conventional characterisation. Both the measurement time and the measurement effort could be significantly reduced. Assuming extensive prior knowledge of the ME sensor system, the acceleration of the measurement time is at least a factor of 7. It simplified filter design in comparison to discrete measurement points, which can, e.g., not anticipate slight changes in the resonance frequency due to interference fields.

### Author Statement

**Research funding:** This work was supported by the German Research Foundation (Deutsche Forschungsgemeinschaft, DFG) through the projects B1 and B9 of the Collaborative Research Centre CRC 1261 Magnetoelectric Sensors: From Composite Materials to Biomagnetic Diagnostics. **Conflict of interest:** Authors state no conflict of interest. **Informed consent:** The conducted research is not related to either human or animal use.

## References

- [1] Elzenheimer E, Bald C, Engelhardt E, Hoffmann J, Hayes P, Arbustini J, et al. Quantitative Evaluation for Magnetoelectric Sensor Systems in Biomagnetic Diagnostics. *Sensors*. 2022;22(3):1018.
- [2] Hoffmann J, Elzenheimer E, Bald C, Hansen C, Maetzler W, Schmidt G. Active Magnetoelectric Motion Sensing: Examining Performance Metrics with an Experimental Setup. *Sensors*. 2021;21(23):8000.
- [3] Elzenheimer E, Hayes P, Thormählen L, Engelhardt E, Zaman A, Quandt E et al. Investigation of Converse Magnetoelectric Thin Film Sensors for Magnetocardiography. *IEEE Sensors Journal*. 2023;23(6):5660-5669.
- [4] Durdaut, P. Ausleseverfahren und Rauschmodellierung für magnetoelektrische und magnetoelastische Sensorsysteme. Shaker Verlag, 2020:67-70.
- [5] Jahns R, Knöchel R, Greve H, Woltermann E, Lage E, et al. Magnetoelectric sensors for biomagnetic measurements. In *Proceedings of the 2011 IEEE International Symposium on Medical Measurements and Applications*. 2011:107110.
- [6] Durdaut P, Wolframm H, Höft M. Low-Frequency Magnetic Noise in Statically-Driven Solenoid for Biasing Magnetic Field Sensors, *arXiv*. 2020:1-6.
- [7] Wolframm H, Höft M. Vorrichtung mit einem Magnetfeldgenerator und Verfahren zur Bereitstellung einer Spulenordnung, European Patent Office (2023), Patent pending.